IEEE Photonics Journal
An IEEE Photonics Society Publication

Adaptive-Modulation-Enabled WDM Impairment Reduction in Multichannel Optical OFDM Transmission Systems for Next-Generation PONs

Volume 2, Number 2, April 2010

E. Giacoumidis
J. L. Wei
X. L. Yang
A. Tsokanos
J. M. Tang

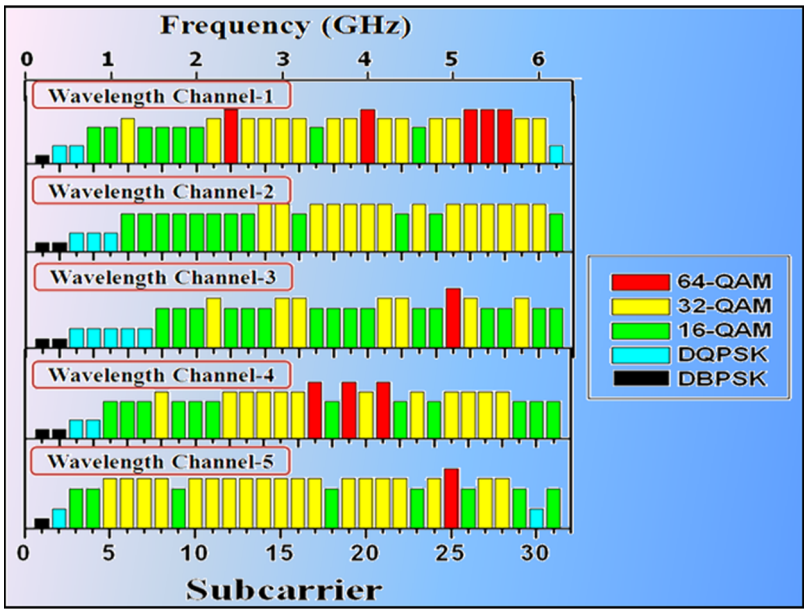

DOI: 10.1109/JPHOT.2010.2044403
1943-0655/$26.00 ©2010 IEEE

Adaptive-Modulation-Enabled WDM Impairment Reduction in Multichannel Optical OFDM Transmission Systems for Next-Generation PONs

E. Giacoumidis, J. L. Wei, X. L. Yang, A. Tsokanos, and J. M. Tang

School of Electronic Engineering, Bangor University, LL57 1UT Bangor, U.K.

DOI: 10.1109/JPHOT.2010.2044403
1943-0655/$26.00 ©2010 IEEE

Manuscript received January 22, 2010; revised February 14, 2010. First published Online March 2, 2010. Current version published March 16, 2010. This work was supported in part by the European Community's Seventh Framework Program (FP7/2007-2013) within the project Information and Communication Technology (ICT) ALPHA under Grant agreement 212 352 and in part by The Royal Society Brian Mercer Feasibility Award. The work of J. L. Wei was also supported by the School of Electronic Engineering, Bangor University. Corresponding author: J. M. Tang (e-mail: j.tang@bangor.ac.uk).

Abstract: The transmission performance of multichannel adaptively modulated optical orthogonal frequency-division multiplexing (AMOOFDM) signals is investigated numerically, for the first time, in optical-amplification-free and chromatic-dispersion-compensation-free intensity-modulation and direct-detection systems directly incorporating modulated distributed feedback (DFB) lasers (DMLs). It is shown that AMOOFDM not only significantly reduces the nonlinear wavelength-division multiplexing (WDM) impairments induced by the effects of cross-phase modulation and four-wave mixing but also effectively compensates for the DML-induced frequency chirp effect. In comparison with conventional modulated optical orthogonal frequency-division multiplexing (OFDM), which uses an identical signal modulation format across all the subcarriers, AMOOFDM improves the maximum achievable signal transmission capacity of a central WDM channel by a factor of 1.3 and 3.6 for 40- and 80-km standard single-mode fibers, respectively, with the corresponding dynamic input optical power ranges being extended by approximately 5 dB. In addition, AMOOFDM also causes the occurrence of cross-channel complementary modulation format mapping among various WDM channels, leading to considerably improved transmission capacities for all individual WDM channels.

Index Terms: Optical fiber communication, orthogonal frequency-division multiplexing (OFDM), single-mode fiber (SMF), wavelength-division multiplexing (WDM).

1. Introduction

In recent years, wavelength-division-multiplexed passive optical networks (WDM-PONs) have gained overwhelming research and development interests, as WDM-PONs are capable of offering a large number of excellent features including, for example, high-quality data service with guaranteed wide bandwidth, large split ratio, aggregated traffic backhauling, simplified network architecture, and enhanced end user privacy [1], [2]. Of various proposed WDM-PON architectures, extended-reach dense WDM-PONs (ER-DWDM-PONs) have been regarded as a promising strategy for high-capacity next-generation PONs (NG-PONs), since ER-DWDM-PONs not only preserve all the aforementioned key features associated with conventional WDM-PONs but also enable the convergence of optical access networks and metropolitan area networks [3], thus resulting in a significant reduction in the number of equipment interfaces and network elements. For

practical deployment of ER-DWDM-PONs, the most critical challenges are cost-effectiveness and flexibility [4].

To achieve cost-effective ER-DWDM-PONs, intensity modulation and direct detection (IMDD) has been adopted as one of the most important technical solutions due to its great network simplicity and low installation and maintenance cost. In particular, a further considerable cost reduction can also be made if directly modulated distributed feedback (DFB) lasers (DMLs) are employed, because, in comparison with external modulators, the DMLs have salient advantages such as low component cost, compactness, relatively small driving voltage required, and high optical output power. On the other hand, to enhance the transmission capacity and system flexibility of ER-DWDM-PONs with their compatibility with existing time-division-multiplexed PONs (TDM-PONs) still being preserved to transparently support legacy services, optical orthogonal frequency-division multiplexing (OOFDM) [4], [5] has been considered to be one of the strongest contenders, since OOFDM has unique and inherent capabilities of realizing high spectral efficiency [6] and providing, in both the frequency and time domains, dynamic allocation of broad bandwidth among various end users, as well as reducing network complexity due to its resistance to linear dispersion impairments and full use of mature digital signal processing (DSP) [7].

Compared with conventional OOFDM, which employs an identical signal modulation format across all the subcarriers, the use of adaptively modulated OOFDM (AMOOFDM) can further improve, in a cost-effective manner, signal transmission capacity, network flexibility, and performance robustness [8]. These properties are extremely valuable for ER-DWDM-PONs. In AMOOFDM, the modulation format taken on a subcarrier within a symbol can be adjusted according to the characteristics of a given transmission system, i.e., a high (low) modulation format is used on a subcarrier experiencing a high (low) signal-to-noise ratio (SNR). Any subcarriers suffering very low SNRs may be dropped completely to avoid the occurrence of a large number of errors on these subcarriers [8].

Therefore, it is greatly beneficial if use is made of the advanced AMOOFDM technique in DML-based IMDD ER-DWDM-PONs without incorporating expensive in-line optical amplification and chromatic dispersion compensation. Unfortunately, to the best of the authors' knowledge, no work has been published that explores such a research topic of great importance. Although the WDM OOFDM transmission performance has been reported in [9] and [10], these works have, however, been focused on long-haul IMDD transmission systems consisting of both external modulators and in-line optical amplifiers. In an IMDD ER-PON architecture involving a DML, the OOFDM transmission performance has been presented in [3]. However, nonlinear WDM impairments have not been addressed, as a single signal channel is considered, and a variable optical attenuator (VOA) is introduced to emulate the possible link loss in ER-WDM-PONs. The utilization of VOAs has been considered to be a fairly common practice for examining the feasibility of implementing a specific transmission technique in conventional low-capacity WDM-PONs with transmission distances of approximately 20 km over standard single-mode fibers (SSMFs), as for such application scenarios, the chromatic dispersion and nonlinear WDM impairments are negligible.

For DML-based IMDD AMOOFDM ER-DWDM-PONs operating at signal bit rates of $>$ 20 Gb/s over $>$ 40-km SSMFs, the above analyses bring up two very interesting open questions, i.e., a) under what conditions do the aforementioned common practice still hold, and b) for cases where the nonlinear WDM impairments are dominant, can an effective technical approach be identified to reduce such impairments? From the practical network design point of view, the provision of answers to these two open questions is very crucial, as these answers may have great potential for offering simple, cost-effective, and accurate solutions for evaluating rigorously the feasibility of implementing the AMOOFDM technique in ER-DWDM-PONs.

This paper is dedicated to exploring theoretically, for the first time, the multichannel AMOOFDM transmission performance in DML-based IMDD ER-DWDM-PONs. In comparison with the conventional OOFDM technique, detailed numerical investigations of the effectiveness of utilizing AMOOFDM in minimizing the nonlinear WDM impairments induced by cross-phase modulation (XPM) and four-wave mixing (FWM) are undertaken. In addition, the validity of the aforementioned common network evaluation practice is also examined.

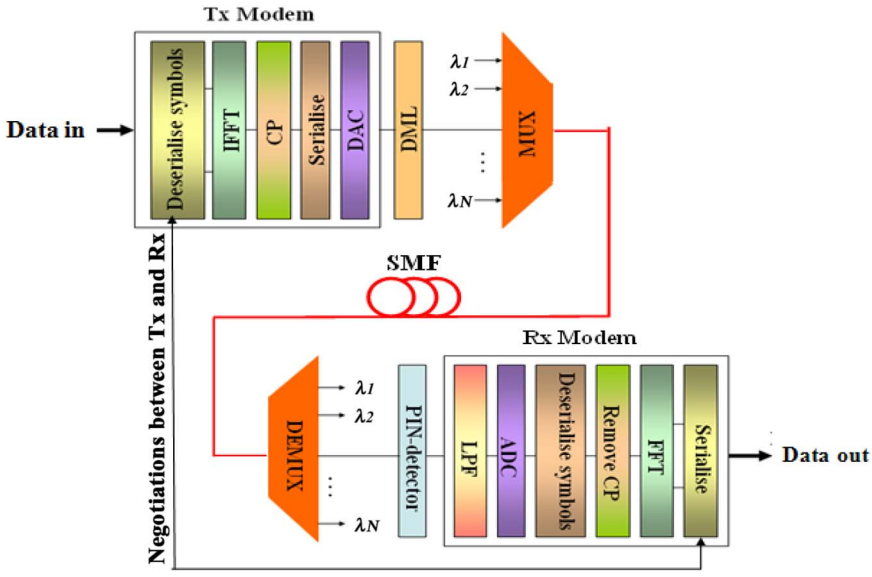

Fig. 1. DML-based IMDD WDM AMOOFDM transmission systems.

2. WDM AMOOFDM Transmission System

2.1. WDM AMOOFDM Transmission System Models

The DML-based IMDD WDM AMOOFDM transmission system considered in this paper is illustrated in Fig. 1, where both in-line optical amplification and chromatic dispersion compensation are not incorporated. In the transmitter, procedures presented in [8] are adopted to simulate the generation of a real-valued baseband OFDM signal in the electrical domain. Combined with a proper DC bias current, the electrical signal having a positive sign is employed to directly drive a DML, from which an AMOOFDM signal is produced at a specific optical wavelength. After the DML, a VOA is employed to adjust the optical signal power at a required level. Making use of different incoming random data sequences, the aforementioned procedures are repeated to generate new WDM channels of different optical wavelengths spaced at a desired frequency interval. All the WDM signals are then aggregated using a multiplexer (MUX), and the combined WDM AMOOFDM signals are finally launched into a simple IMDD SSMF transmission system.

After transmitting through the SSMF, in the receiver, the received WDM signals are separated by a demultiplexer (DEMUX) with a spectral bandwidth being half of the channel spacing. Each separated WDM channel is detected using a square-law photon detector, in which both shot noise and thermal noise are computed following procedures similar to those presented in [8] and [11]. The down-converted electrical signal is processed using an inverse procedure compared with that adopted in the corresponding transmitter, and data is finally recovered for each WDM channel.

To simulate the nonlinear optical properties of a DFB-laser-based DML, here, a lumped DFB laser model developed in [11] is adopted, taking into account a wide range of nonlinear effects such as longitudinal-mode spatial hole burning, linear and nonlinear carrier recombination, and ultrafast nonlinear gain compression. The theoretical DML model also includes the transient frequency chirp effect, which originates from the variation of refractive index with carrier density set by the applied electrical driving current. Both theoretical and experimental investigations [6], [8], [12] have shown that such a frequency chirp plays a dominant role in determining the DML-induced transmission performance degradation. On the other hand, in the theoretical DML model, the DFB adiabatic frequency chirp arising due to the static electrical power dependence of refractive index is not considered, as such a chirp effect is negligible due to the fact that the time-domain electrical driving current is continuous and noise-like and has a relatively small signal extinction ratio [13]. The

validity of the theoretical DML model has been confirmed by excellent agreements with experimental measurements [5], [6]. In addition, the theoretical DML model has also been used successfully in both multimode fiber (MMF)- and SSMF-based transmission systems of various architectures [8], [11], [14], [15].

In this paper, a comprehensive SSMF model used successfully in [8] and [13]–[16] is also employed, taking into account the effects of fiber loss, chromatic dispersion, and polarization dependence of Kerr nonlinearity. In particular, the SSMF model includes self-phase modulation (SPM) in each of two orthogonal linear polarization states: XPM between the two polarization states and polarization-dependent FWM terms [17]. Clearly, for one or more optical signals split into two polarization states, the magnitudes of the XPM and FWM terms also vary with the polarization states of the signals.

2.2. WDM Channel-Bit-Loading Algorithm

As already mentioned in Section 1, AMOOFDM enables the signal modulation format taken on each subcarrier within a symbol to vary, depending upon the characteristics (such as frequency response) of a specific transmission system. Throughout this paper, for each WDM channel, a wide range of signal modulation formats may be utilized, which includes differential binary phase-shift keying (DBPSK), differential quadrature phase-shift keying (DQPSK), and 16-quadrature amplitude modulation (QAM) to 256-QAM. Signal modulation formats taken on individual subcarriers within an AMOOFDM symbol for a specific wavelength channel determine the signal line rate of the wavelength channel. The signal line rate of each WDM channel is computed by

$$R_j = \frac{r_{sj} \sum_{k=1}^{N_{sj}-1} n_{kj}}{2N_{si}(1 + C_{pj})} \tag{1}$$

where j is the index of the WDM channel. $N_{sj} - 1$ is the total number of data-bearing subcarriers in the positive frequency bins, n_{kj} is the total number of binary bits conveyed by the kth subcarrier within one symbol period, r_{sj} is the sampling rate of an analog-to-digital converter (ADC)/digital-to-analog converter (DAC) employed in the jth WDM channel, and C_{pj} is the cyclic prefix parameter defined in [8], [11]. Through negotiations between the transmitter and the receiver in the initial stage of establishing a transmission link, the signal capacity of the jth WDM channel can be maximized by assigning the highest possible signal-modulation format on each subcarrier. This operation is conducted by monitoring the total bit-error rate (BER) of the jth WDM channel, i.e., BER_{Tj}, and its corresponding subcarrier BER, i.e., BER_{kj}, both of which are defined as

$$\mathrm{BER}_{Tj} = \frac{\sum_{k=1}^{N_{sj}-1} En_{kj}}{\sum_{k=1}^{N_{sj}-1} Bit_{kj}} \tag{2}$$

$$\mathrm{BER}_{kj} = \frac{En_{kj}}{Bit_{kj}} \tag{3}$$

where En_{kj} is the total number of errors detected over the entire data sequence adopted in the jth WDM channel, and Bit_{kj} is the total number of transmitted binary bits of the data sequence adopted in the jth WDM channel. Both En_{kj} and Bit_{kj} are for the kth subcarrier. It should be noted that the signal line rate computed using (1) is considered to be valid only when the corresponding $\mathrm{BER}_{Tj} = 1.0 \times 10^{-3}$ is satisfied.

For a given WDM AMOOFDM transmission system, the WDM channel-bit-loading algorithm adopted in numerical simulations is described as followings:

1) A single channel located in the center of the WDM window is first transmitted through the system. Through negotiations between the transmitter and the receiver according to the total

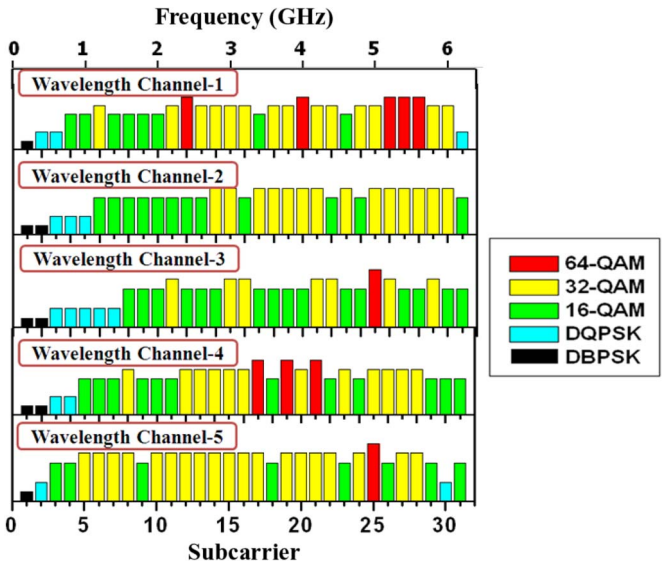

Fig. 2. Signal modulation format distribution across all the subcarriers of five WDM channels with the same polarization states. Cross-channel complementary modulation format mapping is shown.

channel BER and the corresponding subcarrier BER, the highest modulation format taken on each subcarrier within a symbol is identified. Any subcarriers suffering very low SNRs may be dropped completely if the corresponding BERs are still very large, even if they are encoded using DBPSK. Such negotiations are essential for the following two reasons: i) An IMDD SSMF transmission system has a Gaussian-shaped frequency response profile, which narrows rapidly with increasing transmission distance [6], [13]–[16]; and ii) the DFB frequency chirp considerably distorts the system frequency-response profile [6], [8].

2) The signal-modulation formats identified above are applied on the corresponding subcarriers of each of the remaining WDM channels. A combined WDM signal is thus produced and then transmitted through the transmission system.
3) After transmission, for each of the WDM channels, the signal-modulation formats are adjusted independently according to their individual total channel BER and subcarrier BER. These WDM signals are then recombined and transmitted over the same system.
4) Step 3 repeats until a maximum signal capacity at $\mathrm{BER}_T \approx 1.0 \times 10^{-3}$ is achieved for each individual WDM channel.

As discussed in Sections 3–5, the joint manipulation of signal modulation format taken on different subcarriers for all the WDM channels is to effectively reduce the FWM-induced WDM impairments, thus leading to a considerably increased transmission capacity for each WDM channel, compared with that obtained using the conventional OOFDM technique.

It is also worth pointing out that, in the WDM channel bit-loading algorithm, an identical electrical power for each nondropped subcarrier is adopted, regardless of the modulation format used. In comparison with a complex bit and power-loading algorithm widely used in digital subscriber line (DSL) systems [18], the present algorithm gives rise to a very similar signal capacity and, more importantly, significantly reduces the execution time. The reduction in execution time is of great importance, owing to the extremely complexity of the simultaneous maximization of signal modulation formats over several WDM channels.

As an example, a representative modulation format distribution across all the subcarriers is illustrated in Fig. 2 for five WDM AMOOFDM channels after passing through a DML-based IMDD 40-km SSMF transmission system.

In Sections 4 and 5, to demonstrate the effectiveness of AMOOFDM in IMDD WDM systems, the transmission performance of the conventional OOFDM technique is also presented, in which an

identical signal modulation format is taken on each subcarrier within a symbol for each individual WDM channel. The selected modulation format is at the highest possible level to ensure that the BER_T better than 1.0×10^{-3} is still satisfied.

2.3. Simulation Parameters

Five 50-GHz equally spaced WDM channels are considered with the central channel being positioned at 1550 nm. These channels have identical optical powers launched into the SSMF systems. For each individual WDM channel, a total number of 64 (2 Ns) subcarriers are utilized, of which 31 subcarriers carry real data, and one contains no power. The remaining 32 subcarriers are the complex conjugate of the aforementioned 32 subcarriers to enforce Hermitian symmetry in the input facet of the inverse fast Fourier transform (IFFT). The cyclic prefix parameter is taken to be 25% [8]. The ADC/DAC operates at a 12.5-GS/s sampling rate [8], which gives rise to a sampling time duration of 80 ps. Detailed explorations of the influence of quantization and clipping noise on the transmission performance of the AMOOFDM signals have been undertaken in [19], in which an optimum 7-bit resolution and an optimum clipping ratio of 13 dB are identified for signal-modulation formats up to 256-QAM. Therefore, these identified optimum parameter values are adopted in this paper.

All the parameters adopted for both the SSMFs and DFBs can be found in [8] and [11], respectively. In particular, the DFB operating conditions of a 30-mA bias current and a 15-mA peak-to-peak driving current are adopted, which are the optimum values for IMDD SSMF systems with transmission distances of interest of this paper [8]. In the receiver, a *p-i-n* photo-detector is employed having a quantum efficiency of 0.8 and a sensitivity of -19 dBm [corresponding to a 10-Gb/s non-return-to-zero (NRZ) data for a BER_T of 1.0×10^{-9}].

3. Cross-Channel Complementary Modulation Format Mapping

To demonstrate the effectiveness of the WDM channel-bit-loading algorithm described in Section 2, and to gain an in-depth understanding of the results presented in the following sections, discussions are first made of distributions of signal modulation formats across different subcarriers for five WDM channels with the same signal polarization states at the input of the transmission system. The simulated results are illustrated in Fig. 2 which obtain that the transmission distance and the optical launch power per channel are fixed at 40 km and 0 dBm, respectively.

As expected, Fig. 2 shows that, of all the five WDM channels, wavelength channel 3 has the lowest average signal modulation format level and, thus, the smallest transmission capacity of 18.28 Gb/s, while wavelength channel 1 and wavelength channel 5 have higher average signal-modulation format levels and, thus, larger transmission capacities of 21.72 and 21.56 Gb/s, respectively. While the transmission capacities of wavelength channel 2 and wavelength channel 4 are 19.69 and 20.63 Gb/s, respectively. This arises due to crosstalk induced by FWM among different WDM channels. It is easy to understand that the central channel suffers the strongest crosstalk effect and that such an effect decays with increasing frequency difference from the central channel. As a direct result of the triangle-shaped signal spectral distortion across the entire WDM window, cross-channel complementary modulation format mapping occurs, as seen in Fig. 2, i.e., relatively high-signal-modulation formats are taken on high-frequency subcarriers for wavelength channel 1 and wavelength channel 2, while relatively low-signal-modulation formats are taken on high-frequency subcarriers for wavelength channel 4 and wavelength channel 5. Such a cross-channel complementary nature is possible only when AMOOFDM is applied, indicating that AMOOFDM can mitigate, to some extent, the FWM effect and subsequently leads to improvements in both the overall signal capacity of the entire WDM transmission system and each individual WDM channel capacity, in comparison with the conventional OOFDM technique.

It can also be seen in Fig. 2 that, for each individual WDM channel, relatively low-signal modulation formats appear on both sides of the signal spectrum. The low-modulation formats on the low-frequency subcarriers are due to the *subcarrier* $\times$ *subcarrier* intermixing effect, which takes place upon direct photon detection in the receiver [14], [16], and the low-modulation formats on the

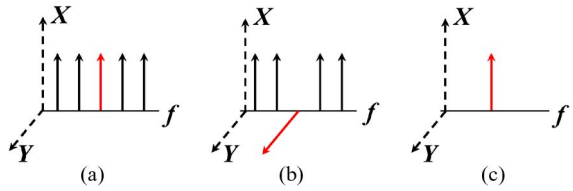

Fig. 3. Polarization states of five WDM channels at the input facet of a transmission system. (a) All x-polarized WDM channels, (b) 4 x-polarized and 1 y-polarized WDM channels, and (c) a single x-polarized channel.

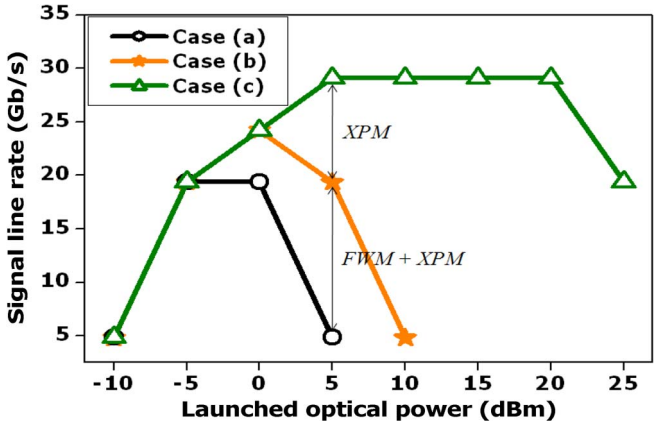

Fig. 4. Transmission capacity versus optical launch power over DML-based 40-km SSMF systems. The conventional OOFDM technique using identical modulation formats across all the subcarriers are used for Case (a), Case (b), and Case (c) defined in Fig. 3.

high-frequency subcarriers are mainly because of the effects of the DML-induced frequency chirp and system frequency response roll-off [6], [14], [15].

As the FWM effect causes the central channel to have the worst transmission performance among all the WDM channels, only the transmission performance of the central channel is, therefore, presented in all the following sections.

4. Adaptive-Modulation-Induced Reduction in WDM Impairments

To investigate in detail the impacts of the effects of XPM and FWM on the transmission performance of the worst-case central WDM channel, numerical simulations are undertaken for three different polarization conditions at the input facet of a transmission system, as shown in Fig. 3: Case (a) consists of five x-polarized WDM channels, the central channel experiences the XPM, and FWM effects; in Case (b), the central channel is set at y-polarization, and the other four WDM channels remain at x-polarization. Such a signal polarization arrangement leads to the central channel suffering from the XPM effect only, which is one third weaker than that in Case (a) [17]. Finally, Case (c) just includes a single x-polarized channel, where the XPM and FWM impairments do not exist. It should be pointed out that the similar SPM effect is always present in each WDM channel for all three different cases.

The signal line rate of the central WDM channel versus optical launch power per channel is plotted in Fig. 4 for a DML-based 40-km IMDD transmission system subject to three polarization conditions defined in Fig. 3. To highlight the XPM and FWM effects only, in simulating Fig. 4, the conventional OOFDM technique is considered for all the WDM channels. The developing trends of signal transmission capacity shown in Fig. 4 are very similar to those observed in [9]. By comparing the three different curves shown in Fig. 4, it is clear that XPM plays a dominant role in determining the maximum achievable transmission performance of the central channel for optical launch powers larger than 0 dBm. Compared with the XPM effect, the FWM effect is relatively weaker, which,

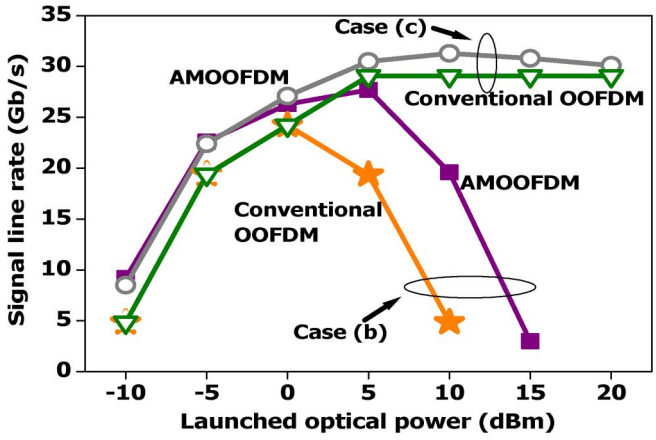

Fig. 5. Signals capacity versus optical launch power over DML-based 40-km IMDD SMF systems subject to different polarization launch conditions. Case (b) and Case (c) defined in Fig. 3.

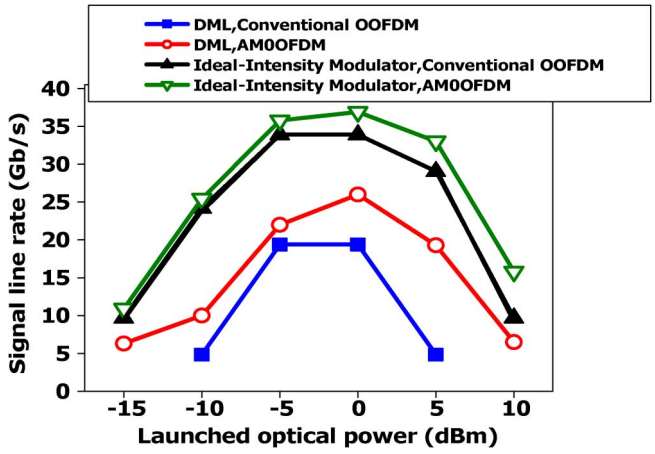

Fig. 6. Transmission capacity versus optical launch power for AMOOFDM and conventional OOFDM over 40-km IMDD systems including and excluding DMLs. Case (a) is considered.

however, increases exponentially with decreasing channel spacing. On the other hand, for optical launch powers less than 0 dBm, the XPM- and FWM-induced nonlinear WDM impairments are negligible, implying that the use of VOAs in evaluating the WDM network performance is sufficiently accurate. However, for optical launch powers beyond such a value, the linear network evaluation approach is not valid. In Case (c), the reduction in signal transmission capacity for optical launch powers of $>$ 20 dBm is contributed by the SPM effect.

It is very interesting to note that the use of AMOOFDM can considerably reduce the nonlinear WDM impairments induced by XPM and FWM, as seen in Figs. 5 and 6. In Fig. 5, performance comparisons are made between AMOOFDM and conventional OOFDM for Case (b) and Case (c), and in Fig. 6, similar comparisons are made for Case (a). These figures show that, as a direct result of cross-channel complementary modulation format mapping presented in Section 3, the adaptive-modulation-enabled performance enhancement is more pronounced for the WDM case than that for the single-channel case. In addition, compared with conventional OOFDM, in the WDM nonlinearity-limited performance region, AMOOFDM not only improves the maximum achievable signal bit rate by a factor of $>$ 1.3 but also extends the optimum optical launch power by about 5 dB.

Apart from the reduction in the FWM-induced crosstalk effect via cross-channel complementary modulation format mapping, the significantly improved transmission performance observed in Figs. 5 and 6 is also due to the fact that the AMOOFDM can also produce a signal peak-to-average

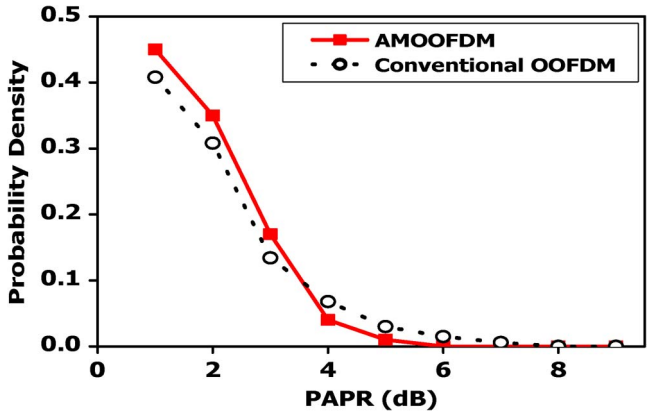

Fig. 7. Signal peak occurrence probability density versus PAPR for AMOOFDM and conventional OOFDM. The optical launch power is fixed at 5 dBm, and the transmission link is 40 km.

power ratio (PAPR) lower than that corresponding to conventional OOFDM. This is because AMOOFDM decreases the probability of independently modulated subcarriers being added up coherently by the IFFT. This statement is confirmed in Fig. 7, where the signal peak occurrence probability density versus PAPR is plotted for AMOOFDM and conventional OOFDM. The signal peak occurrence probability density ρ is defined as

$$\rho = \frac{n_{\text{PAPR}}}{n_T} \tag{4}$$

where n_{PAPR} is the total number of signal peaks occurring within a power variation range of 1 dB with respect to a specific PAPR value, and n_T is the total number of signal peaks occurring within the entire PAPR range. It should be noted that, in calculating Fig. 7, use is made of the optical signals emerging at the output facet of a 40-km transmission system at an input optical power of 5 dBm.

It can be seen in Fig. 7 that, in comparison with conventional OOFDM, AMOOFDM produces more signal peaks in a low-PAPR region of < 4 dB and fewer signal peaks in a high-PAPR region of > 4 dB. As the XPM-related optical phase is proportional to the intensity of the other signal channel travelling simultaneously over the same fiber, a small PAPR gives rise to the reduced XPM effect, as seen in Figs. 5 and 6. In addition, it is also easy to understand that a low PAPR also results in a reduction in the FWM effect [17].

According to the above analyses, it is very easy to understand that the effectiveness of utilizing adaptive modulation to compensate for the nonlinear WDM impairments can be enhanced considerably with increasing transmission distance. As an example, in comparison with conventional OOFDM, for a transmission distance of 80 km, numerical simulations show that AMOOFDM can improve the maximum achievable signal bit rate of the central channel by a factor of 3.6, which is approximately three times higher than that corresponding to the 40-km transmission distance case.

5. DML Frequency Chirp Compensation

Apart from the aforementioned significant reduction in the XPM and FWM effects, use can also be made of AMOOFDM to effectively compensate for the DML-induced frequency chirp effect, as shown in Fig. 6, where comparisons of the transmission performances for Case (a) are made between a DML and an ideal intensity modulator to distinguish clearly the impacts of the DML-induced frequency chirp effect. The output optical signal from the ideal intensity modulator $S_o(t)$ can be written as

$$S_o(t) = \sqrt{S_e(t)} \tag{5}$$

where $S_e(t)$ is the total electrical current applied to the DML. It is shown in Fig. 6 that the DML-induced frequency chirp effect degrades dramatically the transmission performance. This is in very good agreement with results presented in [8] and [15]. More importantly, compared with conventional OOFDM, AMOOFDM is capable of improving considerably the transmission performance across the entire optical launch power range, especially for optical launch powers of > 0 dBm. Such behaviors can be explained by considering the fact that the DML frequency chirp distorts considerably the optical signal spectrum via lifting up the high-frequency spectral region by approximately 10 dB after transmitting through 40-km SSMFs [8]. AMOOFDM can fully utilize all parts of the spectrum by taking low-signal-modulation formats on the most distorted spectral regions, as illustrated in Fig. 2. This causes the transmission performance enhancement over the entire optical launch power region of interest of the present paper. Moreover, AMOOFDM can also reduce the signal PAPR, resulting in a small electrical signal current variation and, thus, a low DML frequency chirp [12]. Such an effect is more significant for high optical launch powers. It is also worth pointing out that the DML-induced frequency chirp increases the walk-off effect between different wavelength channels, whose contribution to the FWM effect is, however, negligible, as the AMOOFDM signals have noise-like time-domain waveforms with approximated Gaussian probability density functions [8], [11], [13].

6. Conclusion

The transmission performance of multichannel AMOOFDM signals has been explored numerically, for the first time, in DML-based IMDD SSMF systems without involving in-line optical amplification and chromatic dispersion compensation for ER-DWDM-PONs. It has been shown that AMOOFDM cannot only significantly reduce the nonlinear WDM impairments induced by the XPM and FWM effects but can also effectively compensate for the frequency chirp effect associated with the DMLs. Investigations have also revealed that, in comparison with conventional OOFDM, AMOOFDM improves the maximum achievable signal transmission capacity of a central WDM channel by a factor of 1.3 and 3.6 for 40-km and 80-km SSMFs, respectively, with the corresponding dynamic input optical power range being extended by approximately 5 dB. In addition, the adaptive-modulation-enabled performance enhancement is more pronounced for optical launch powers of > 0 dBm. Furthermore, AMOOFDM also enables the occurrence of cross-channel complementary modulation format mapping, leading to considerably improved transmission capacities for each individual WDM channel and the entire WDM transmission system.

The present work suggests that AMOOFDM is promising for practical implementation in ER-DWDM-PONs. From the practical implementation point of view, the maximum achievable signal-transmission capacity of the system of interest of the paper is mainly limited by the following three factors including properties of DACs/ADCs adopted, DML-induced relatively small-signal extinction ratio, and subcarrier intermixing upon direct photon detection in the receivers. It is also worth mentioning that following the successful experimental demonstration of 11.25-Gb/s real-time end-to-end OOFDM transceivers [20], experimental verifications of the theoretical predictions are currently being undertaken, and results will be reported elsewhere in due course.

References

[1] T. Koonen, "Fiber to the home/fiber to the premises: What, where, and when," *Proc. IEEE*, vol. 94, no. 5, pp. 911–934, May 2006.
[2] P. W. Shumate, "Fibre-to-the-home: 1977-2007," *J. Lightw. Technol.*, vol. 26, no. 9, pp. 1093–1103, May 2008.
[3] C.-W. Chow, C.-H. Yeh, C.-H. Wang, F.-Y. Shih, C.-L. Pan, and S. Chi, "WDM extended reach passive optical networks using OFDM-QAM," *Opt. Express*, vol. 16, no. 16, pp. 12096–12101, Aug. 2008.
[4] D. Qian, N. Cvijetic, J. Hu, and T. Wang, "Optical OFDM transmission in metro/access networks," presented at the Optical Fiber Communication/Nat. Fiber Optic Engineers Conf. (OFC/NFOEC), San Diego, CA, 2009, Paper OMV1.
[5] N. E. Jolley, H. Kee, R. Rickard, J. Tang, and K. Cordina, "Generation and propagation of a 1550 nm 10 Gb/s optical orthogonal frequency division multiplexed signal over 1000 m of multimode fibre using a directly modulated DFB," presented at the Optical Fiber Communication/Nat. Fiber Optic Engineers Conf. (OFC/NFOEC), Anaheim, CA, 2005, Paper OFP3.

[6] X. Q. Jin, R. P. Giddings, E. Hugues-Salas, and J. M. Tang, "Real-time demonstration of 128-QAM-encoded optical OFDM transmission with a 5.25 bit/s/Hz spectral efficiency in simple IMDD systems utilizing directly modulated DFB lasers," *Opt. Express*, vol. 17, no. 22, pp. 20484–20493, Oct. 2009.
[7] R. P. Giddings, X. Q. Jin, and J. M. Tang, "First experimental demonstration of 6 Gb/s real-time optical OFDM transceivers incorporating channel estimation and variable power loading," *Opt. Express*, vol. 17, no. 22, pp. 19727–19738, Oct. 2009.
[8] J. M. Tang and K. A. Shore, "30-Gb/s signal transmission over 40-km directly modulated DFB-laser-based single-mode-fibre links without optical amplification and dispersion compensation," *J. Lightw. Technol.*, vol. 24, no. 6, pp. 2318–2327, Jun. 2006.
[9] A. J. Lowery, L. B. Du, and J. Armstrong, "Performance of optical OFDM in ultra-long-haul WDM lightwave systems," *J. Lightw. Technol.*, vol. 25, no. 1, pp. 131–138, Jan. 2007.
[10] D. Qian, J. Yu, J. Hu, L. Zhou, L. Xu, and T. Tang, "10 Gb/s WDM-SSB-OFDM transmission over 1000 km SSMF using conventional DFB lasers and direct-detection," *Electron. Lett.*, vol. 44, no. 3, pp. 223–225, Jan. 2008.
[11] J. M. Tang, P. M. Lane, and K. A. Shore, "High-speed transmission of adaptively modulated optical OFDM signals over multimode fibres using directly modulated DFBs," *J. Lightw. Technol.*, vol. 24, no. 1, pp. 429–441, Jan. 2006.
[12] J. A. P. Morgado and A. V. T. Cartaxo, "Directly modulated laser parameter optimisation for metropolitan area networks utilizing negative dispersion fibres," *IEEE J. Sel. Topics Quantum Electron.*, vol. 9, no. 5, pp. 1315–1324, Sep./Oct. 2003.
[13] J. L. Wei, X. L. Yang, J. M. Tang, and R. P. Giddings, "Colourless adaptively modulated optical OFDM transmitters using SOAs as intensity modulators," *Opt. Express*, vol. 17, no. 11, pp. 9012–9027, May 2009.
[14] J. L. Wei, X. Q. Jin, and J. M. Tang, "The influence of directly modulated DFB lasers on the transmission performance of carrier suppressed single sideband optical OFDM signals over IMDD SMF systems," *J. Lightw. Technol.*, vol. 27, no. 13, pp. 2412–2419, Jul. 2009.
[15] E. Giacoumidis, J. L. Wei, X. Q. Jin, and J. M. Tang, "Improved transmission performance of adaptively modulated optical OFDM signals over directly modulated DFB laser-based IMDD links using adaptive cyclic prefix," *Opt. Express*, vol. 16, no. 13, pp. 9480–9494, Jun. 2008.
[16] X. Zheng, J. L. Wei, and J. M. Tang, "Transmission performance of adaptively modulated optical OFDM modems using subcarrier modulation over SMF IMDD links for access and metropolitan area networks," *Opt. Express*, vol. 16, no. 25, pp. 20 427–20 440, Dec. 2008.
[17] T. Schneider, *Nonlinear Optics in Telecommunications*. New York: Springer-Verlag, 2004.
[18] S. C. J. Lee, F. Breyer, S. Randel, D. Cárdenas, H. P. A. Boom, and A. M. J. Koonen, "Discrete multi-tone modulation for high-speed data transmission over multimode fibres using 850-nm VCSEL," presented at the Optical Fiber Communication/Nat. Fiber Optic Engineers Conf. (OFC/NFOEC), San Diego, CA, 2009, Paper OWM2.
[19] J. M. Tang and K. A. Shore, "Maximizing the transmission performance of adaptively modulated optical OFDM signals in multimode-fiber links by optimizing analog-to-digital converters," *J. Lightw. Technol.*, vol. 25, no. 3, pp. 787–798, Mar. 2007.
[20] R. P. Giddings, X. Q. Jin, E. Hugues-Salas, E. Giacoumidis, and J. M. Tang, "Experimental demonstration of a record high 11.25 Gb/s real-time optical OFDM transceivers supporting 25 km SMF end-to-end transmission in simple IMDD systems," *Opt. Express*, vol. 18, no. 6, pp. 5541–5555, Mar. 2010.